Supplementary Information

Utilizing Hydrogen Underpotential Deposition in CO Reduction for Highly Selective Formaldehyde Production under Ambient Condition

*Libo Yao†, Yanbo Pan†, Xiaochen Shen, Dezhen Wu, Abdulaziz Bentalib, Zhenmeng Peng**

Department of Chemical and Biomolecular Engineering, The University of Akron, Akron, OH 44325, United States.

† These authors contributed equally to this work.

* Corresponding author, e-mail: zpeng@uakron.edu

Table of Contents

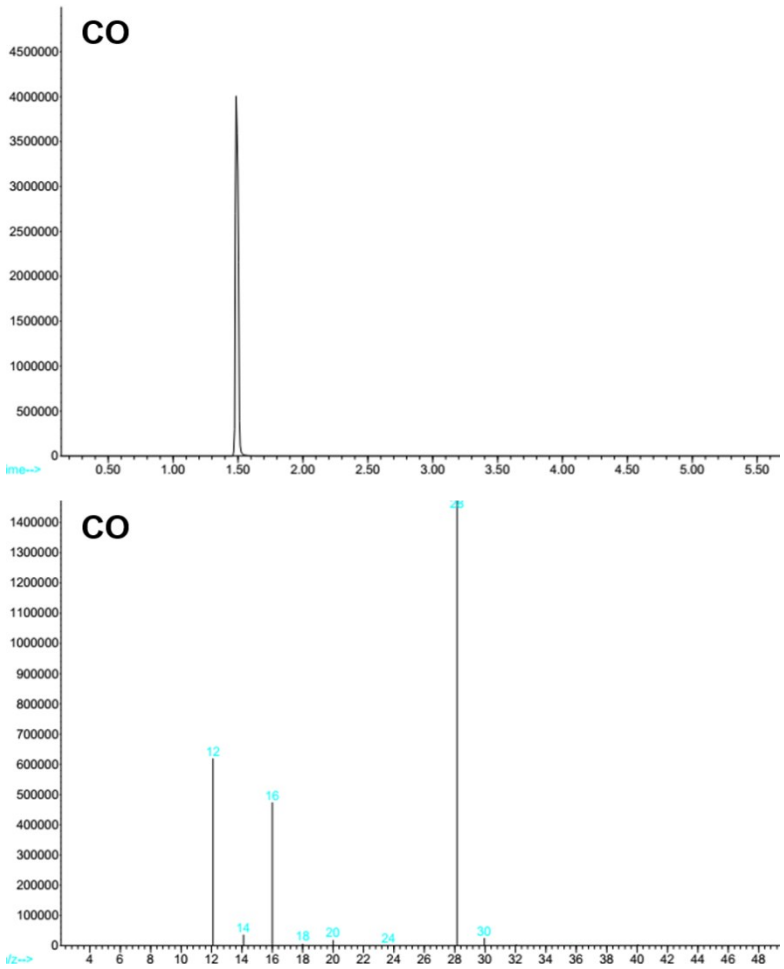

Fig. S1 On-line GC-MSD result of gas product from CORTF reaction under -100 μA cm^{-2}.

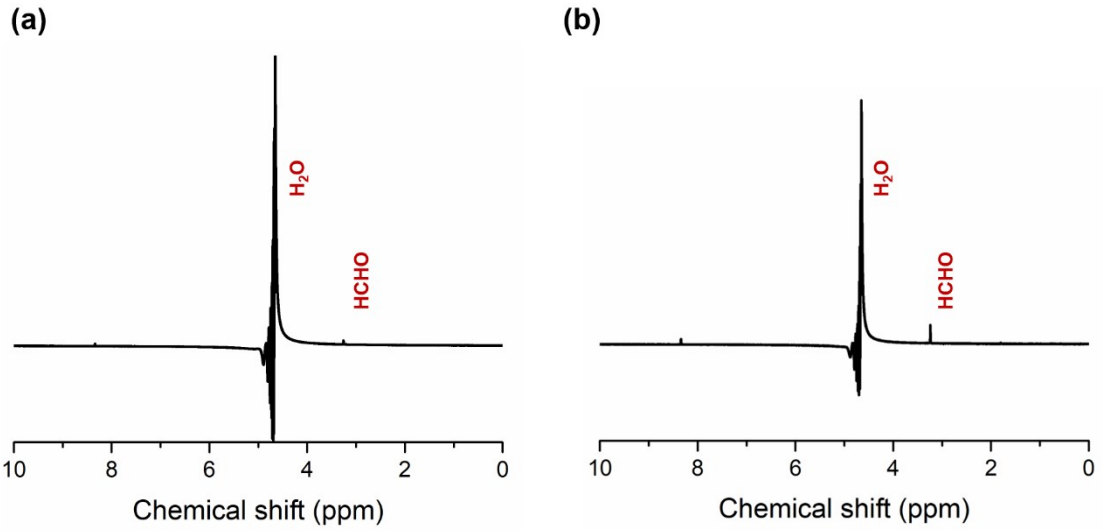

Fig. S2 a, NMR spectrum of liquid product from CORTF reaction under -100 μA cm^{-2}. b, NMR spectrum of 4.17 ppm of HCHO standard solution for comparison purpose. The peak positioned at 8.34 is not identified as any product because it appeared in every NMR spectra, including the HCHO standard solution.

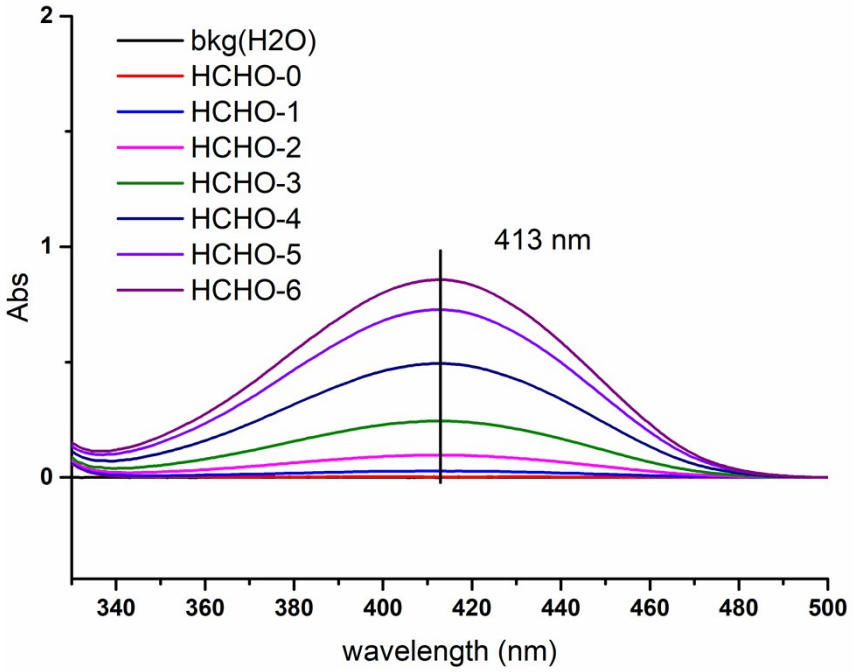

Fig. S3 UV-Vis spectra of HCHO standard samples (0-0 μg/ml, 1-0.083 μg/ml, 2-0.333 μg/ml, 3-0.833 μg/ml, 4-1.667 μg/ml, 5-2.5 μg/ml and 6-2.917 μg/ml)

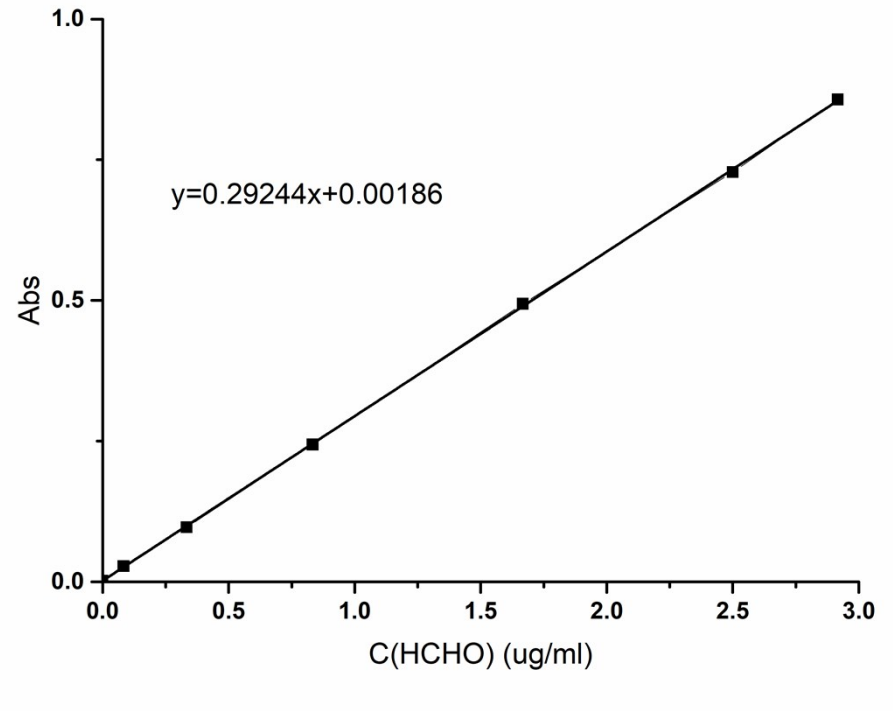

Fig. S4 Working curve for HCHO quantification.

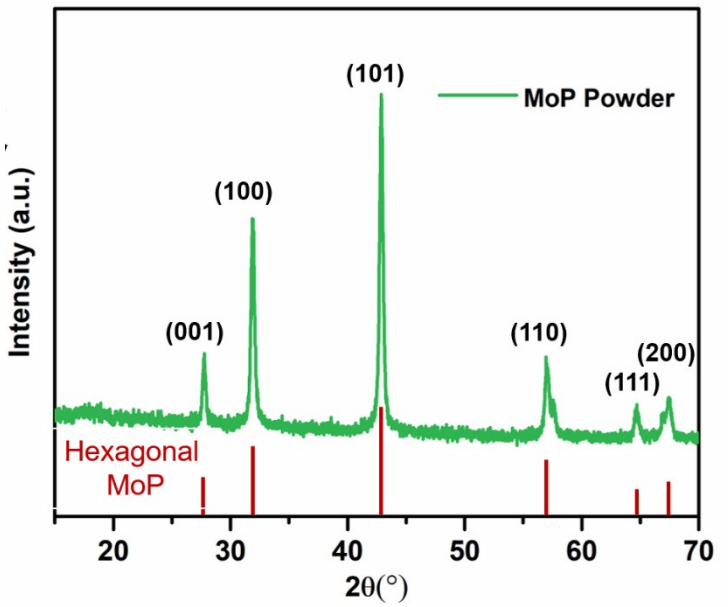

Fig. S5 XRD patterns of MoP powder (ICDD 03-065-6487).

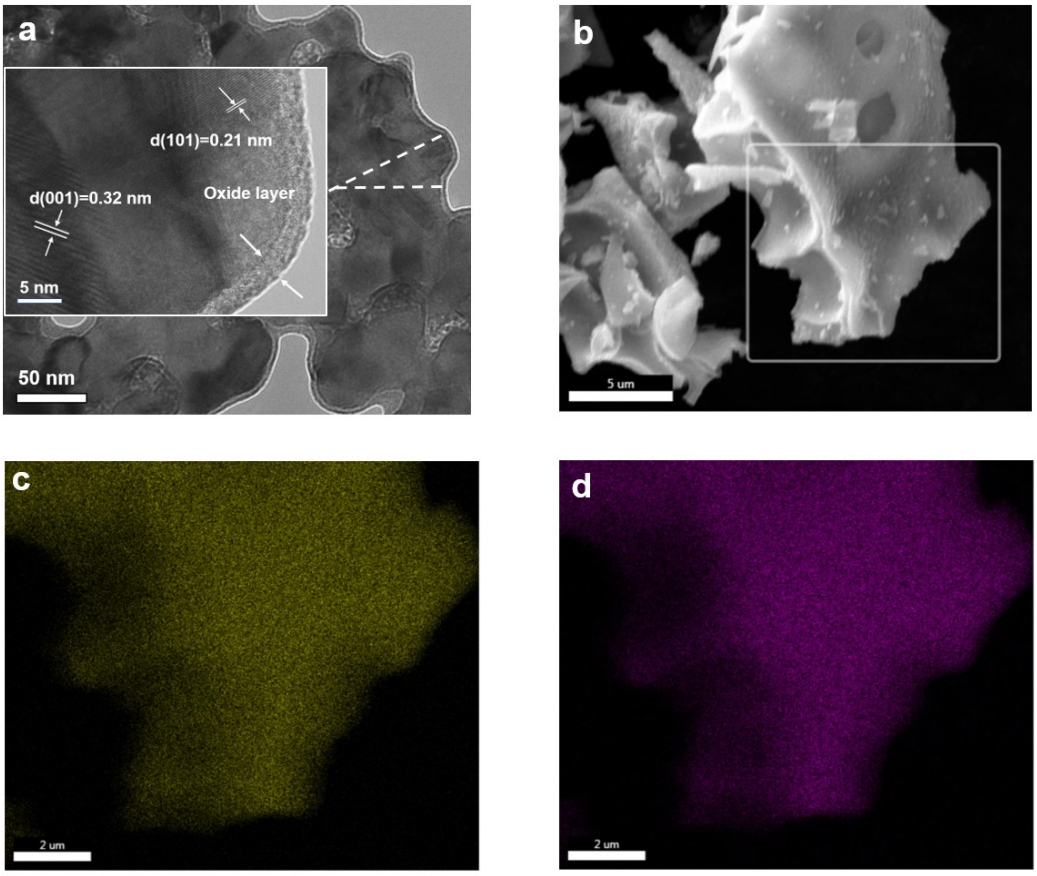

Fig. S6 HRTEM image of MoP (a), SEM image of MoP (b) and EDX mapping images of Mo (c) and P (d).

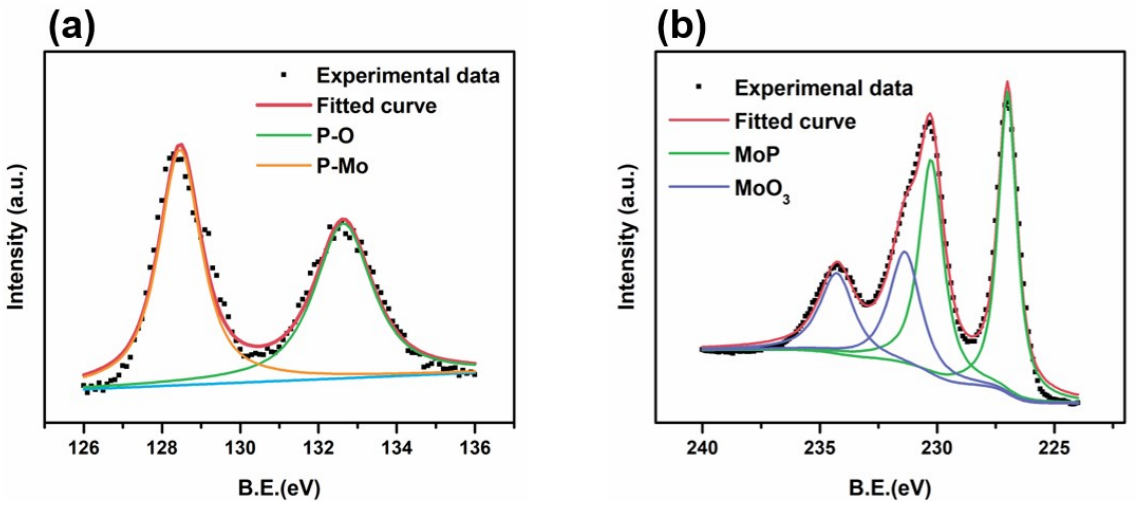

Fig. S7 XPS spectra of **a**, P 2p and **b**, Mo 3d.

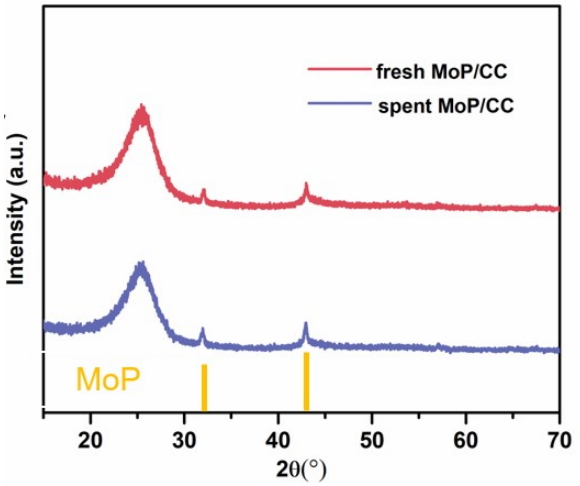

Fig. S8 XRD patterns of MoP/CC before and after CORTF test.

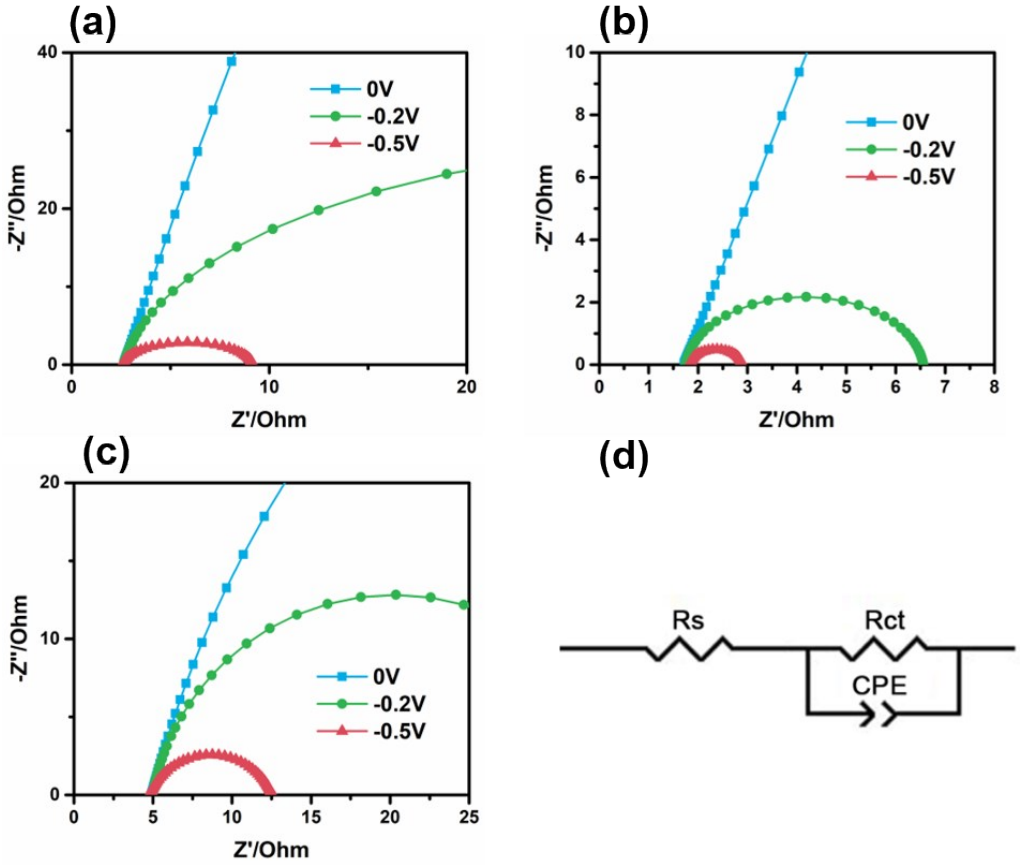

Fig. S9 Electrochemical impedance spectra in CO-saturated electrolyte fitted with equivalent circuit (d): a, 0.5 M KOH; b, 0.5M H_2SO_4 and c, 0.5 M Na_2SO_4.

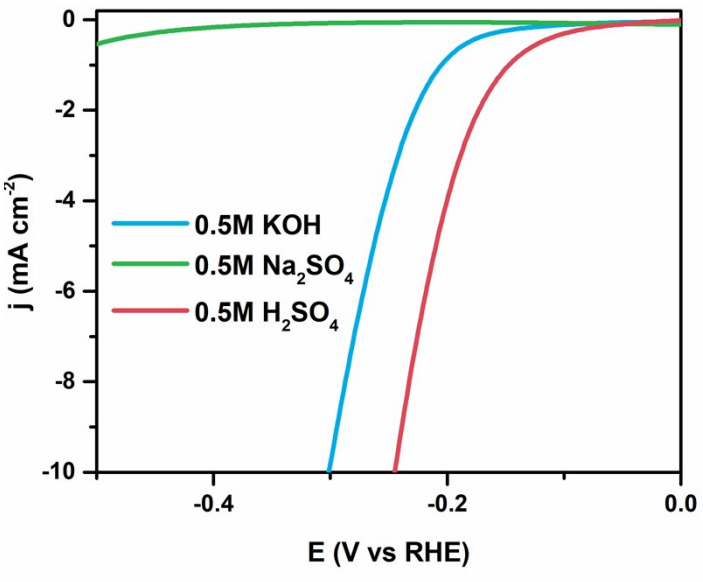

Fig. S10 Polarization curves performed without CO introduction in 0.5 M KOH, H_2SO_4 and Na_2SO_4 electrolytes.

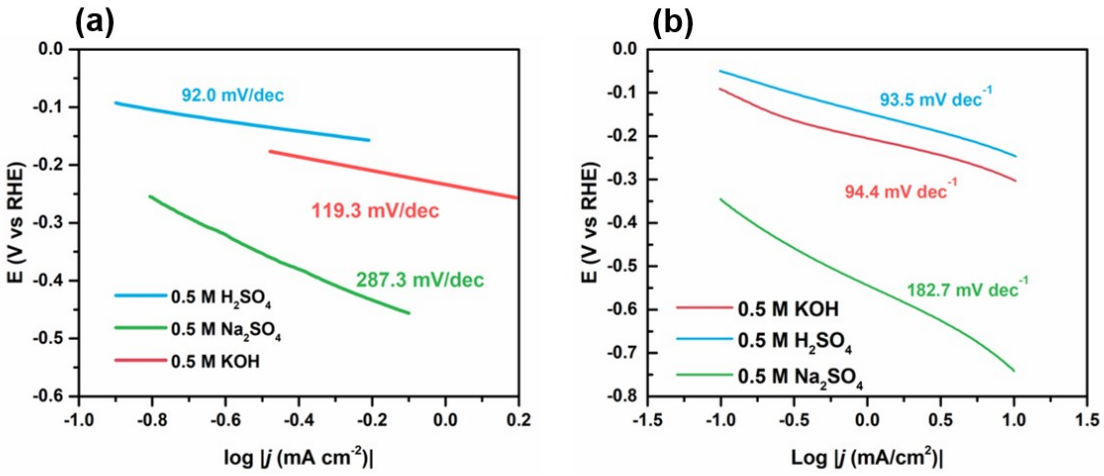

Fig. S11 Tafel plots derived from polarization curves obtained (a) in presence and (b) in absence of CO.

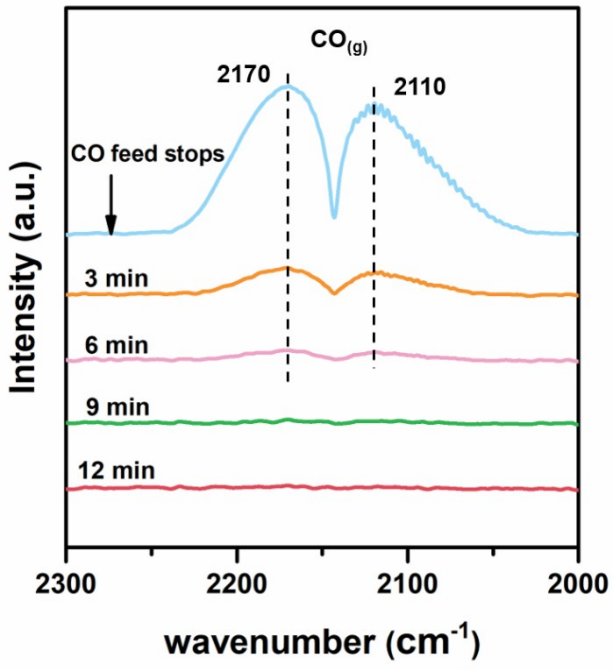

Fig. S12 In situ DRIFTS experiment on CO adsorption ability of MoP powder under room temperature. 0 min was counted when CO feed was switched to Ar for purging. The result shows no adsorbed CO species and the gaseous CO was swiftly swept out by Ar purge.

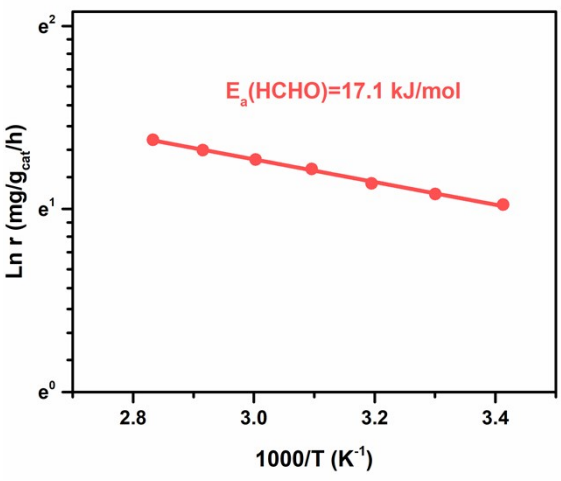

Fig. S13 Apparent activation energy of HCHO (E_a) derived from reaction data in Fig. 2c.

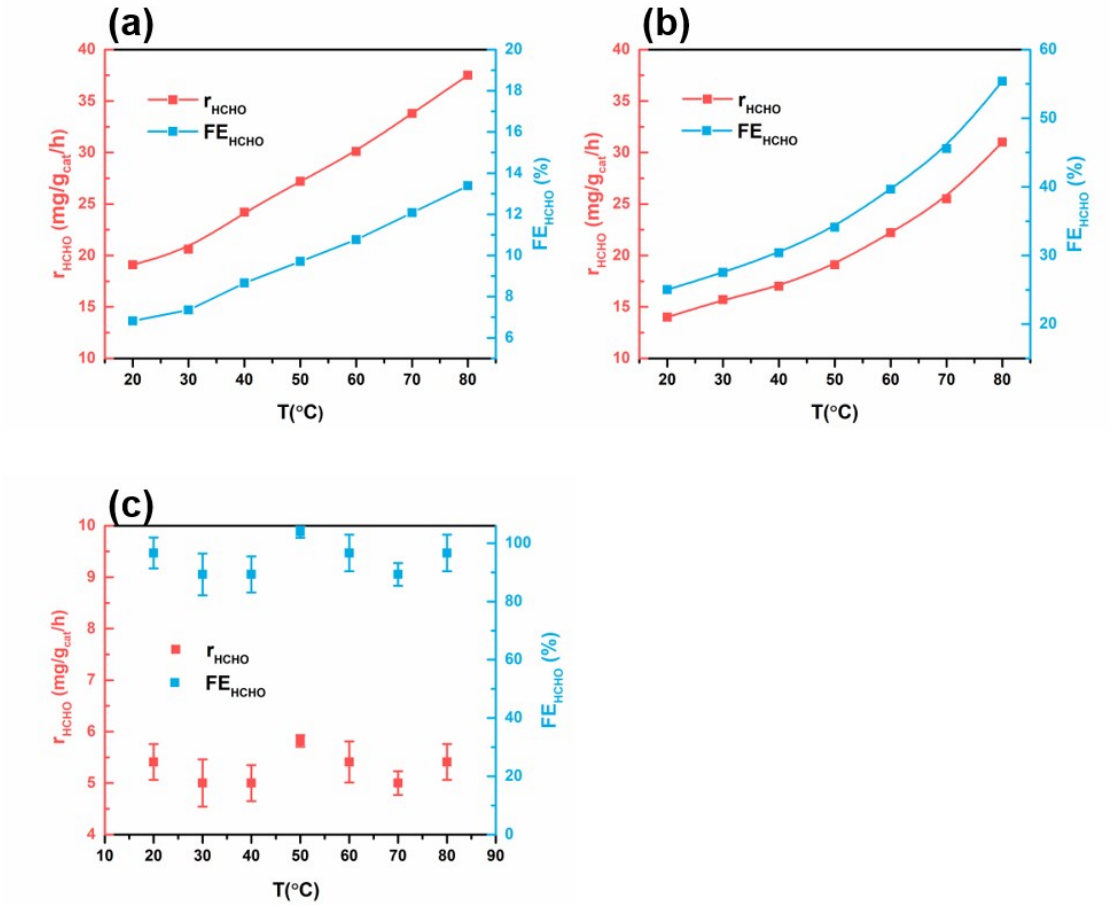

Fig. S14 Temperature dependent r_{HCHO} and FE_{HCHO} obtained under a, -250 μA cm^{-2}, b, -50 μA cm^{-2}, and c, -5 μA cm^{-2}.

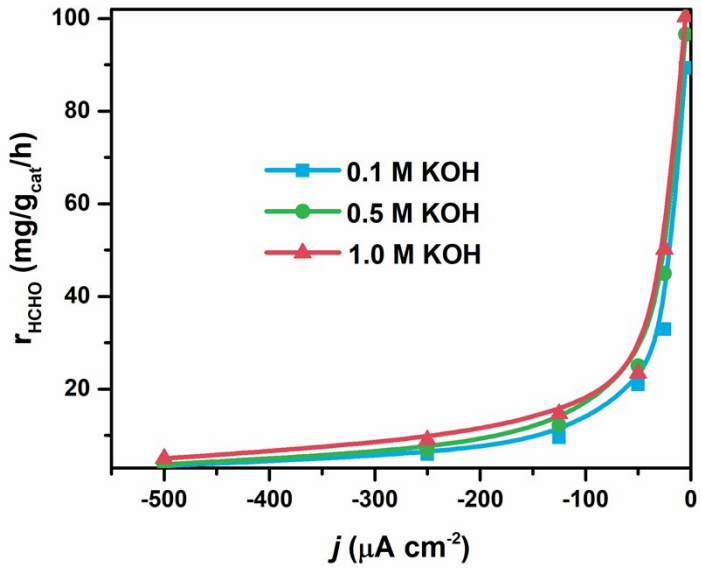

Fig. S15 Effect of KOH concentration on the FE_{HCHO} at various current densities.

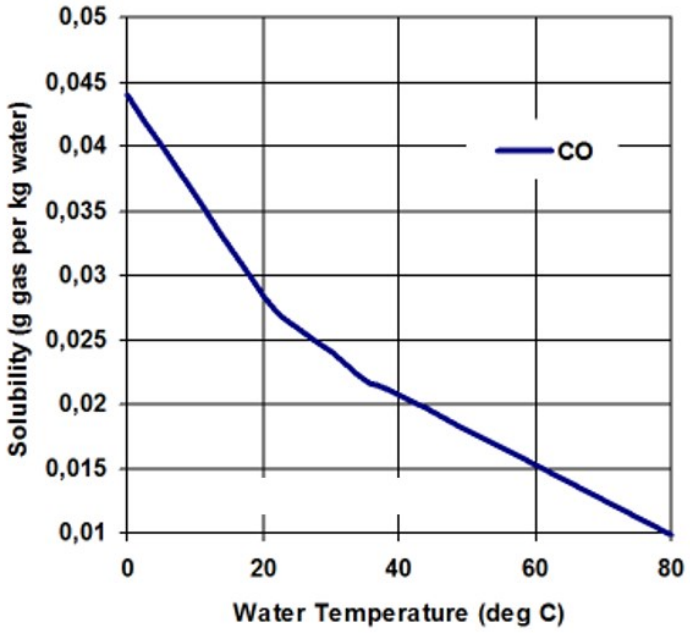

Fig. S16 Solubility of CO in water as a function of temperature. At 25 °C, the saturated concentration of CO is approximately 0.986 mmol/L. Data obtained from Engineering ToolBox, (2008). *Solubility of Gases in Water*. Available at: https://www.engineeringtoolbox.com/gases-solubility-water-d_1148.html.

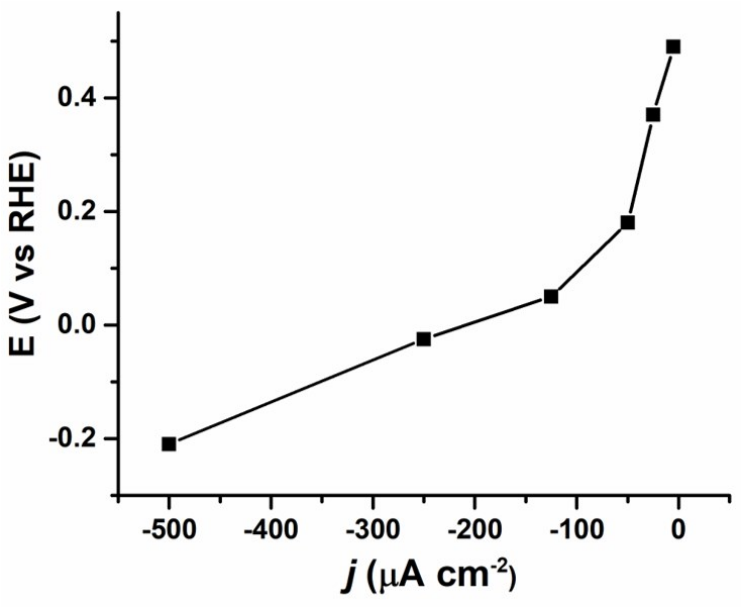

Fig. S17 Correspondence of measured current density as function of potential.

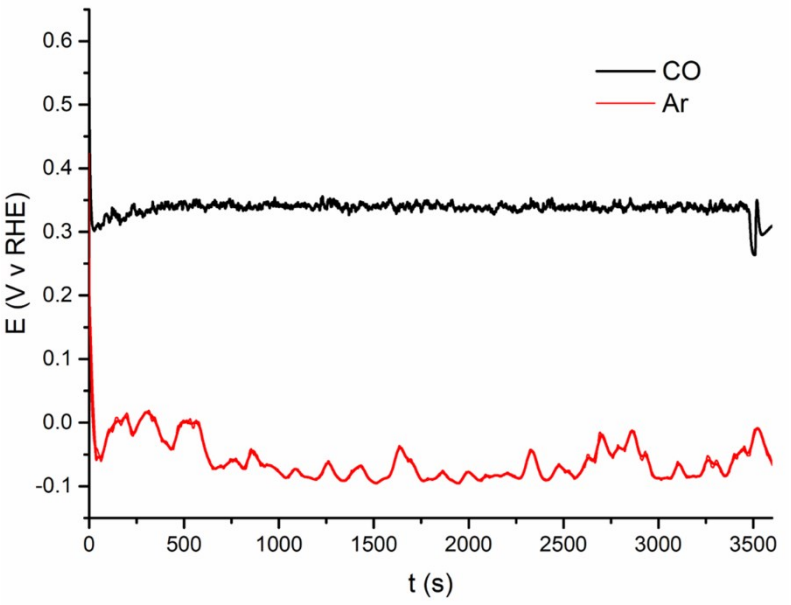

Fig. S18 Comparison of the E-t curves conducted with and without CO under -50 μA cm^{-2}.

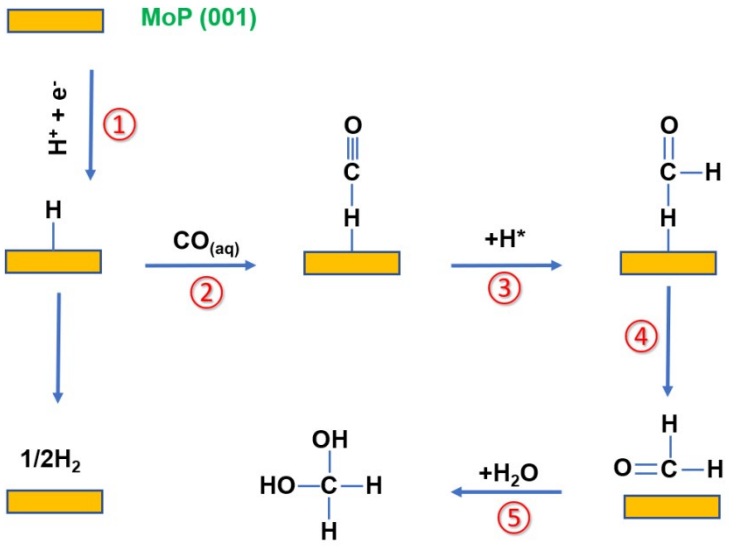

Fig. S19 Proposed reaction pathways for HER and CORTF reactions.

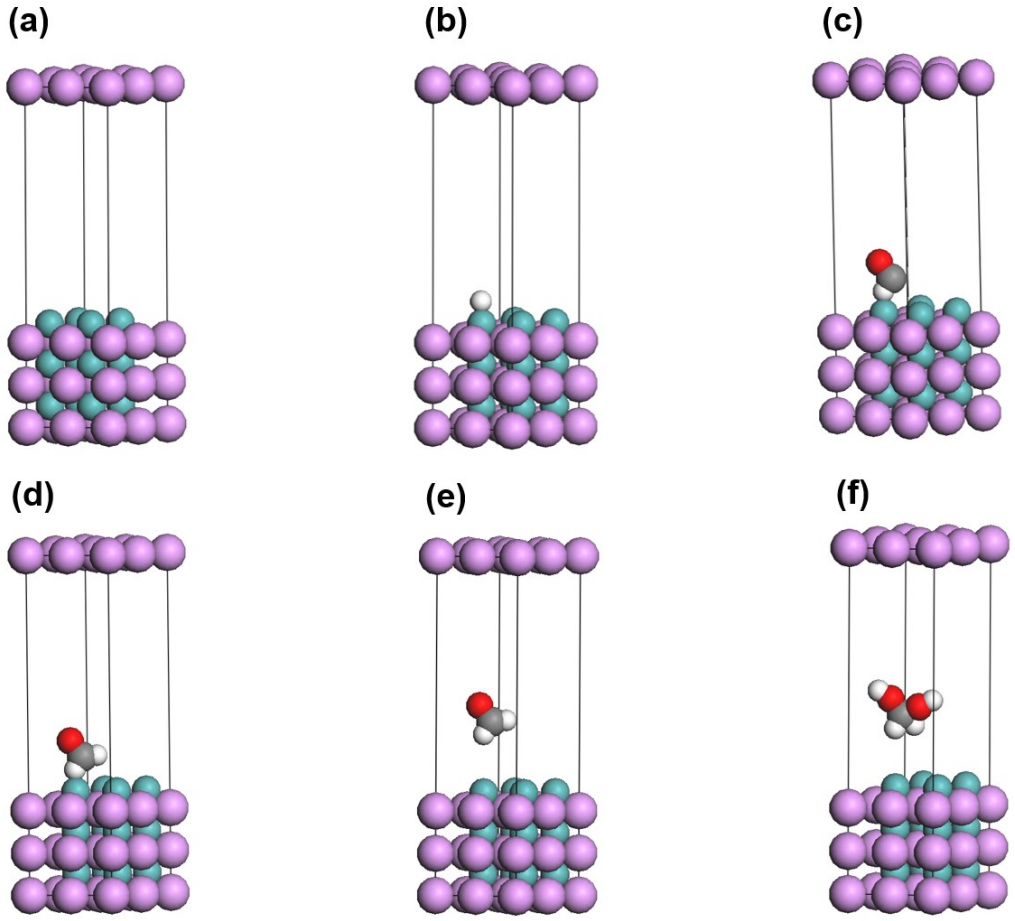

Fig. S20 Models for the structures of reaction intermediates on Mo-terminated MoP (001) surface. a, pristine MoP (001) surface. b, *H. c, *HCO. d, *H_2CO. e, CH_2O and f, CH_4O_2.

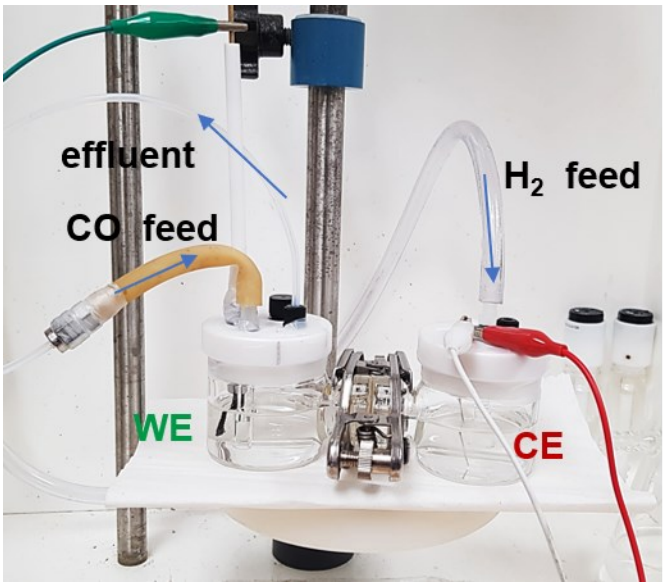

Fig. S21 Photo of the 2-compartment cell used for full cell reaction.

Table S1 Fitting data derived from EIS spectra in 0.5 M H_2SO_4, Na_2SO_4, and KOH electrolytes.

Solution	R_s (Ω)	R_{ct} (Ω)	CPE	
			-T	-P
0.5 M H_2SO_4 E=0 V	1.71	7577	0.0006	0.845
0.5 M H_2SO_4 E=-0.2 V	1.75	4.81	0.0002	0.935
0.5 M H_2SO_4 E=-0.5 V	1.83	1.06	0.0002	0.95
0.5 M Na_2SO_4 E=0 V	4.91	136.3	0.0009	0.85
0.5 M Na_2SO_4 E=-0.2 V	4.98	30.58	0.0008	0.89
0.5 M Na_2SO_4 E=-0.5 V	4.76	7.8	0.002	0.74
0.5 M KOH E=0 V	2.63	3409	0.0047	0.92
0.5 M KOH E=-0.2 V	2.63	62.61	0.0017	0.93
0.5 M KOH E=-0.5 V	2.55	6.65	0.002	0.90

Table S2. Comparison of CORTF performance between present work and the state-of-art technologies.

Catalyst	Technology	Reaction condition		r_{HCHO} ($mg/g_{cat}/h$)	Ref
		Pressure (bar)	T (K)		
MoP	Electrolysis	1	293	16.16	Present work
Pd-Ni/Al_2O_3	Fixed bed	85	313	2.56	2
Ru-Ni/Al_2O_3	Slurry reactor	100	403	0.768	3

Table S3. Gibbs free energies (ΔG) of adsorbates and products. (Calculated based on ΔG=ΔH-TS, data obtained from Ref.1 for Mo-terminated (001) surface.)

Species	ΔG (eV)
*H	-0.31
*HCO	-0.40
*H_2CO	-0.42
CH_2O	0.16
CH_4O_2	-0.07

Reference

(1) Duyar, M.S., Tsai, C., Snider, J.L., Singh, J.A., Gallo, A., Yoo, J.S., Medford, A.J., Abild-Pedersen, F., Studt, F., Kibsgaard, J. and Bent, S.F. A highly active molybdenum phosphide catalyst for methanol synthesis from CO and CO_2. *Angew. Chem. Int. Ed.* **2018**, *57*(46), 15045-15050.

(2) Bahmanpour, A. M.; Hoadley, A.; Tanksale, A. Formaldehyde production via hydrogenation of carbon monoxide in the aqueous phase. Green Chem. 2015, 17, 3500-3507.

(3) Bahmanpour, A. M.; Hoadley, A.; Mushrif, S. H.; Tanksale, A. Hydrogenation of carbon monoxide into formaldehyde in liquid media. ACS Sustain. Chem. Eng. 2016, 4, 3970-3977.